

## Production and Identification of the Ion-Temperature-Gradient Instability

A. K. Sen, J. Chen, and M. Mael

Plasma Research Laboratory, Columbia University, New York, New York 10027

(Received 6 August 1990)

In order to produce and study the ion-temperature-gradient instability, the Columbia Linear Machine has been modified to yield a peaked ion temperature and flattish density profiles. Under these conditions the parameter  $\eta_i (=d \ln T_i / d \ln N)$  exceeded the critical value and a strong instability has been observed. Further identification has been based on observation of the azimuthal and axial wavelengths, and the real frequency, appropriate for the mode.

PACS numbers: 52.35.Kt, 52.35.Mw

Anomalous ion thermal conductivity remains an open physics issue for the present generation of high-temperature tokamaks and future reactor-type tokamaks. One important component of this transport is now widely believed to be due to the ion-temperature-gradient instability ( $\eta_i$  mode).<sup>1-4</sup> However, it has been difficult, if not impossible, to identify this instability *directly* in tokamaks. Therefore, the production and identification of this mode is presently pursued in the simpler and experimentally convenient configuration of the Columbia Linear Machine (CLM).<sup>5</sup> In the CLM a hydrogen plasma, with coincident radial temperature and density gradients, is produced by a  $\mathbf{E} \parallel \mathbf{B}$  discharge source. The machine is approximately 3 m in overall length and has a uniform axial magnetic field. In the past, localized mirrors creating a mirror cell were used for the study of various trapped-particle instabilities as shown in Fig. 1. For the present purpose of producing an ion-temperature-gradient instability which does not depend on trapped particles or curvature drive, we do not energize the mirror coils. The typical parameters of the CLM before modifications are (i)  $N \sim 6 \times 10^8 - 2 \times 10^9 \text{ cm}^{-3}$ ,  $T_e \sim 5-8 \text{ eV}$ ,  $T_i \sim 5 \text{ eV}$ , and  $P_n \sim 7 \times 10^{-7} \text{ Torr}$ ,

without density reduction grids and rf, and (ii)  $N \sim 2 \times 10^8 \text{ cm}^{-3}$ ,  $T_e \sim 10 \text{ eV}$ ,  $T_{i \parallel} \sim 10 \text{ eV}$ ,  $T_{i \perp} \sim 50 \text{ eV}$ , and  $P_n \sim 7 \times 10^{-7} \text{ Torr}$ , with density reduction grids and rf. The other parameters are  $r_p \sim 2.7 \text{ cm}$ ,  $1/r_p L_n \sim 0.27 \text{ cm}^{-2}$ ,  $L_c \sim 50-150 \text{ cm}$ ,  $B_0 = 1 \text{ kG}$ ,  $v_e / \omega^* \sim 0.0015-0.2$ ,  $v_{en} / \omega^* \sim 0.15-0.01$ ,  $v_e / \omega_{Be}, v_e / \omega_{te} \sim v_i / \omega_{Bi}$ ,  $v_i / \omega_{ti} \sim 3 \times 10^{-5} - 10^{-3}$ ,  $\eta_e \sim 1.0-2$ ,  $\eta_i \sim 0$ , and  $\rho_i / r_p \sim 0.2-0.1$ . Therefore the dimensionless parameters of CLM, relevant to electrostatic microinstabilities, can clearly range from those of TFTR, DIII, and JET to very collisionless plasmas of future reactor-type tokamaks. It is clear that for our present purpose the only adequate parameter is  $\eta_i$ . This parameter has to be increased beyond the critical value  $\eta_{ic}$  for the instability, which is generally estimated to be of the order of 1. The methods and modifications to accomplish this are described below. The rf for the parameter set (ii), generated by a slot antenna, produced a flat ion-temperature profile with  $\eta_i \sim 0$ . Therefore we adopt the machine configuration leading to the parameter set (i), supplemented by the heating scheme described below.

The parameter  $\eta_i$  can be increased either by flattening the density gradient or by increasing the ion-temperature gradient (from zero). It must be emphasized that even for zero density gradient, one must have an appropriate ion-temperature gradient to excite this instability, which is a temperature-gradient-driven mode. A "feathered" screen installed at the entrance of the experimental region can significantly lower the density gradient. Various electromagnetic ion-cyclotron-resonance-heating antennas have failed to produce appropriately peaked temperature profiles. Launching electrostatic ion cyclotron waves directly near the plasma axis sometimes succeeded in producing moderately peaked  $T_{i \perp}$  profiles, but failed to excite any instability. This led to an examination of the consequences of only transverse heating and creation of

$$\eta_{i \perp} = d \ln T_{i \perp} / d \ln N \gg \eta_{i \parallel} = d \ln T_{i \parallel} / d \ln N \sim 0.$$

A theory of ion-temperature-gradient instability with anisotropic  $\eta_i$  has been developed,<sup>6</sup> which indicates the

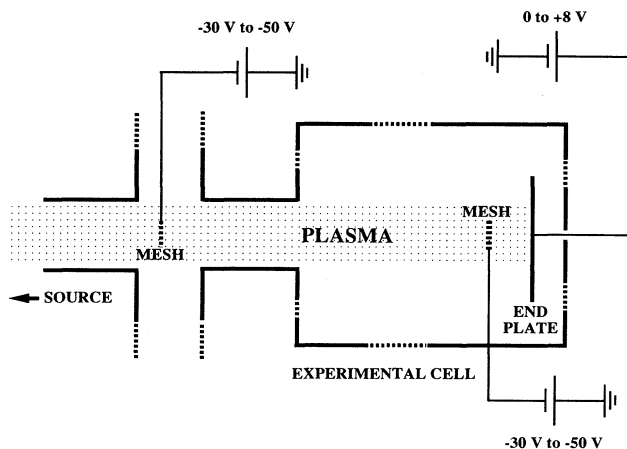


FIG. 1. Schematic of the parallel-ion-acceleration scheme.

critical role of  $\eta_{i\parallel}$  and a secondary role of  $\eta_{i\perp}$ . This motivated the development of a scheme for parallel heating of ions.

The basic idea of the scheme is to accelerate the ions from the plasma source before these enter the experimental cell as shown in Fig. 1. The acceleration parallel to the magnetic field is achieved via a 70% transparent tungsten mesh at the end of the plasma column, both biased to  $-30$  to  $-50$  V. Lastly, the terminating end plate has a bias of  $+4$  to  $+8$  V to contain the heated ions, while the typical plasma potential is  $-6$  to  $-8$  V. Thermalization in the high-neutral-pressure transition region, subsequent to acceleration, produces parallel ion heating roughly in the region covered by the accelerating meshes (or radii 1 and 0.6 cm). This leads to a peaked  $T_{i\parallel}$  profile. Furthermore, the mesh in the transition region reduces the density in the central core and helps to reduce the density gradient. Therefore the biased mesh can act as both a density flattening and parallel-temperature-peaking device and can produce high values of  $\eta_{i\parallel}$ .

Profiles of plasma parameters in the absence of parallel ion heating (with no accelerating bias on the meshes) are shown in Fig. 2(a). The electron density, electron

temperature, ion temperature, and electrostatic potential are measured by Langmuir probes, parallel and transverse energy analyzers, and emissive probes, respectively. It is seen that  $\nabla T_{i\perp} \sim 0$ ,  $\nabla T_{i\parallel} \sim 0$  over the entire plasma core. As the parallel ion heating is turned on (with accelerating bias on the meshes), profiles change as shown in Fig. 2(b). It is clearly seen that  $T_{i\perp}$  profiles remain essentially flat, but  $T_{i\parallel}$  profiles have developed strong gradients in the vicinity of the accelerator mesh location. This is a clear consequence of the fact that the biased meshes can only accelerate ions in the parallel direction and yield an enhanced parallel temperature, while leaving the transverse ion temperature unaltered. We can now examine the fluctuation spectra in the plasma with and without ion parallel heating. In the absence of parallel heating, we have the profiles of Fig. 2(a) where  $\nabla T_{i\perp} \sim 0$ ,  $\nabla T_{i\parallel} \sim 0$ . The corresponding density fluctuation spectrum (from the fluctuating ion saturation current drawn by a Langmuir probe) is shown in Fig. 3(a). Under these circumstances, we really do not expect any  $\eta_i$  mode. However, there is one spectral feature at 27 kHz, which is a  $\mathbf{E}_0 \times \mathbf{B}_0$  rotationally driven mode, always present in our machine with a radial equilibrium electric field produced by the potential ( $\Phi$ ) profile in Fig.

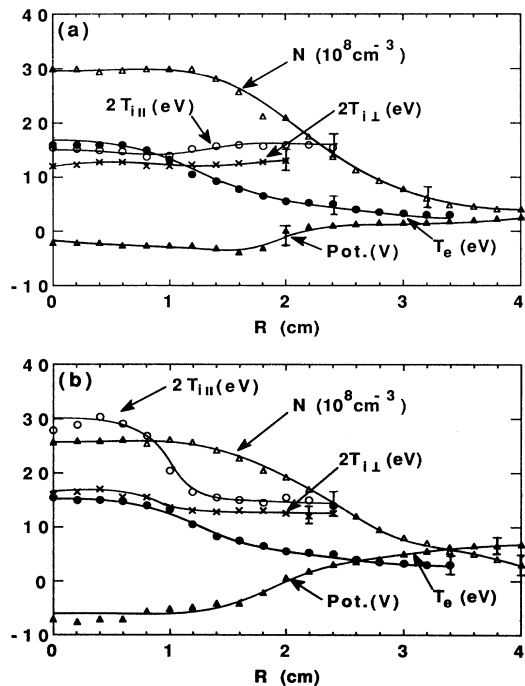


FIG. 2. Radial profiles of plasma parameters.  $N$ ,  $T_{i\parallel}$ ,  $T_{i\perp}$ ,  $T_e$ , and Pot are equilibrium plasma density, parallel ion temperature, transverse ion temperature, electron temperature, and potential, respectively. (a) Profiles without parallel heating of the ions (i.e., zero bias on the accelerating meshes). (b) Profiles with parallel heating of the ions (i.e.,  $-50$ -V bias on both meshes).

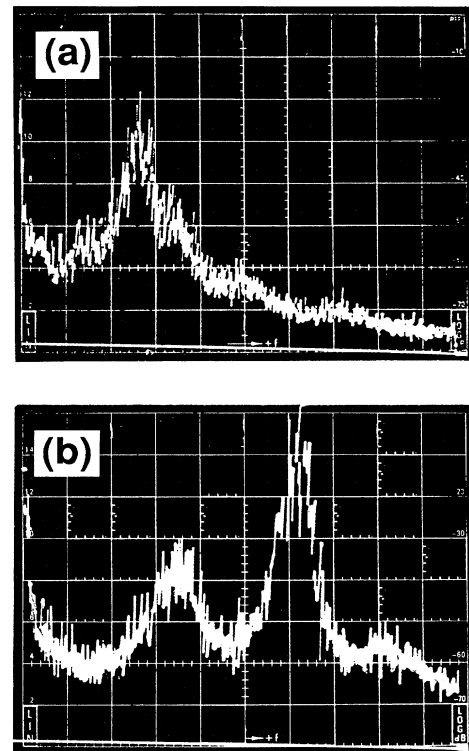


FIG. 3. Density fluctuation spectra. (a) Spectrum without parallel ion heating, corresponding to the profiles of Fig. 2(a). 10 kHz per division. (b) Spectrum with parallel ion heating, corresponding to the profiles of Fig. 2(b). 10 kHz per division.

2(a). As the parallel heating is turned on (via the biases on the meshes), the profiles change as shown in Fig. 2(b), and now  $\nabla T_{i\perp} \sim 0$ , and  $\nabla T_{i\parallel}$  is quite large. The corresponding fluctuation spectrum is shown in Fig. 3(b). The usual  $\mathbf{E}_0 \times \mathbf{B}_0$  rotationally driven mode is still there at a slightly higher frequency of 35 kHz, but a new mode is clearly visible at 62 kHz. Under a variety of plasma conditions, this new mode correlates with the existence of a strong  $\nabla T_{i\parallel}$  and is therefore considered as a strong candidate for  $\eta_i$  mode.

The azimuthal mode number and axial wavelength of both modes are determined via cross correlation of two appropriately placed Langmuir probes. The results show that the first mode at 27–35 kHz is  $m=1$  and  $\lambda_{\parallel} \gg L$ , which conforms with the notion that it is a  $\mathbf{E}_0 \times \mathbf{B}_0$  rotationally driven flute. The second mode at 62 kHz is  $m=2$  and  $\lambda_{\parallel} \sim 330 \text{ cm} \sim 2L$ , and is necessarily a driftlike mode and not a flute mode. A detailed shooting code analysis using the actual profiles shows that the  $m=1$  rotationally driven flute mode is unstable in both the absence and presence of parallel heating. However, the  $m=2$  rotationally driven flute is stable in both cases. Therefore on the basis of the experimental evidence of finite- $\lambda_{\parallel}$  measurements and computational results of  $\mathbf{E} \times \mathbf{B}$  rotational flute stability, the  $m=2$  second mode at 62 kHz is judged to be very likely a  $\eta_i$  mode. Lastly, the radial localization of the  $m=1$  mode is observed to be much broader than that of the  $m=2$  mode, indicative of the difference between a global flutelike mode and a more localized driftlike mode.

We now discuss the  $\eta_i$  stability character of this mode by examining the marginal stability criteria. For  $\nabla n \approx 0$  and  $\nabla T_{i\perp} \approx 0$  one needs to use the inverse-temperature-gradient scale-length parameter  $\delta_{i\parallel} = (dT_{i\parallel}/dr)/T_{i\parallel}$ . Then using the results developed in Ref. 6 we calculate the critical temperature-gradient scale length and compare with the experimental value as follows: theoretical,  $(L_{T_{i\parallel}})_{\text{crit}} = (\delta_{i\parallel \text{crit}})^{-1} = 2.2$  ( $m=1$ ) and 4.0 ( $m=2$ ) cm; experimental,  $\langle L_{T_{i\parallel}} \rangle_{\text{expt}} \sim 2.4$  cm.

The experimental measurement of  $L_{T_{i\parallel}}$  has been averaged over the mode width to yield  $\langle L_{T_{i\parallel}} \rangle$ . From the above numbers for theoretical and experimental ion-temperature-gradient scale lengths, it is clear that the  $m=1$  mode is marginally stable, but the  $m=2$  mode will be strongly unstable. This is in clear consonance with the experimental evidence of the emergence of a  $m=2$  mode, whenever  $\nabla T_{i\parallel}$  is strong as shown in Fig. 3(b). A preliminary numerical solution of the radially nonlocal problem (to be published in a future publication) supports this conclusion.

Lastly, we vary the fraction of heating ions confined in the experimental cell by varying the confining potential created by the (positive) dc bias on the terminating end plate. Figure 4 shows the resulting fluctuation spectra as a function of increasing fraction of heated ions with temperature gradient. This clearly indicates the  $\eta_i$  nature of

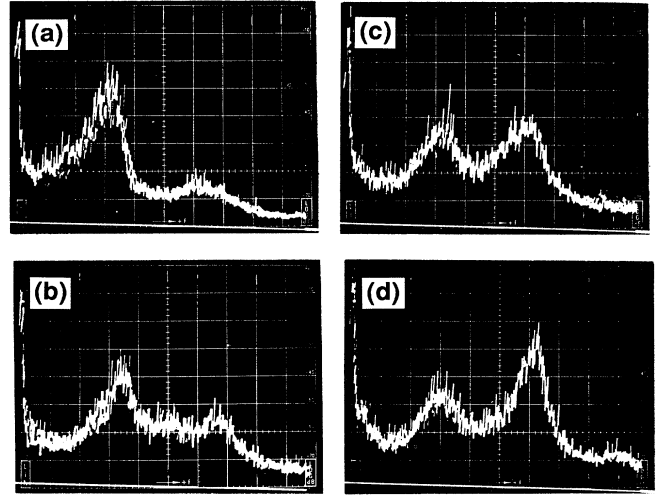


FIG. 4. Mode dependence on fraction of heated ions with temperature gradient  $\nabla T_{i\parallel}$ . (a)–(d), density fluctuation spectra for increasingly larger fraction of heated ions with strong temperature gradient. 10 kHz per division.

the instability.

We now discuss the real frequency of the modes. In Figs. 2(b) and 3(b) the  $m=1$  rotationally driven flute-like mode has negligible real frequency in the plasma frame. Therefore its frequency in the laboratory frame will be

$$\omega_r(\text{flute}) \sim m \langle \omega_E \rangle \sim \langle \omega_E \rangle \text{ for } m=1,$$

where  $\langle \omega_E \rangle$  is the mode-averaged  $\mathbf{E} \times \mathbf{B}$  rotational frequency. This is in the direction of electron diamagnetic drift frequency in our machine. For our experimental parameters the computed rotational frequency is

$$\langle \omega_E \rangle_{\text{th}} = \int_{\text{mode width}} \frac{1}{r} \frac{E(r)}{B} dr \sim 25\text{--}30 \text{ kHz } (m=1).$$

This is in fair agreement with the experimental observation of 27 to 35 kHz. On the other hand, for the  $\eta_i$  mode, we have the real frequency as

$$\omega_r(\eta_i) = \omega_r^{\text{plasma}} + \mathbf{k} \cdot \mathbf{V}_0,$$

where  $\mathbf{V}_0$  is the total plasma macroscopic velocity and  $\mathbf{k}$  is the wave vector. As  $\mathbf{V}_0$  consists of a small axial flow velocity  $\mathbf{V}_{\text{flow}}$  and  $\mathbf{E}_0 \times \mathbf{B}_0$  velocity, we have

$$\omega_r(\eta_i) = \omega_r^{\text{plasma}} + k_{\parallel} V_{\text{flow}} + m \langle \omega_E \rangle.$$

Neglecting the small axial flow velocity and estimating  $\omega_r^{\text{plasma}} \approx -k_{\parallel} V_{\text{thi}}$  from Ref. 6 with  $k_{\parallel} = \pi/L = \pi/150$ , we find

$$\omega_r(\eta_i) \approx m \langle \omega_E \rangle - k_{\parallel} V_{\text{thi}}$$

$$= 2\pi(2 \times 35 - 10) \text{ kHz} \sim 2\pi \times 60 \text{ kHz } (m=2).$$

As the plasma-frame frequency of the  $\eta_i$  mode is a small

negative value (propagating in the ion diamagnetic direction), we should then expect this mode at roughly the second harmonic of the  $\mathbf{E}_0 \times \mathbf{B}_0$  rotational frequency. This is clearly the case as seen in the spectrum of Fig. 3(b). Furthermore, we always see this mode at a frequency slightly *lower* (6–10 kHz) than the second harmonic of the rotational frequency, which is consistent with the propagation of this mode in the ion diamagnetic direction.

In conclusion, we have succeeded in producing and identifying the  $\eta_i$  instability. Its identification has been based on its appearance in conjunction with high  $\nabla T_{i\parallel}$  and low  $\nabla N$  and the fact that the observed mode with wave numbers  $m=2$ ,  $k_{\parallel}=\pi/L$  is predicted to be strongly  $\eta_i$  unstable. Furthermore, as predicted the real frequency of the mode is observed to be in the vicinity of the

second harmonic of the  $\mathbf{E}_0 \times \mathbf{B}_0$  rotation frequency, with a modest downshift in frequency due to the propagation of the mode in the ion diamagnetic direction.

---

<sup>1</sup>S. M. Wolfe and M. Greenwald, Nucl. Fusion **26**, 329 (1986).

<sup>2</sup>D. L. Brower, W. A. Peebles, S. K. Kim, N. C. Luhmann, Jr., W. M. Tang, and P. E. Phillips, Phys. Rev. Lett. **59**, 49 (1987).

<sup>3</sup>R. J. Groebner, W. W. Pfeiffer, F. P. Blau, and K. H. Burrell, Nucl. Fusion **26**, 543 (1986).

<sup>4</sup>B. Coppi, in Proceedings of the Sherwood Theory Conference, 1984 (unpublished), paper 3A3.

<sup>5</sup>G. A. Navratil, J. Slough, and A. K. Sen, Plasma Phys. **24**, 185 (1982).

<sup>6</sup>O. Mathey and A. K. Sen, Phys. Rev. Lett. **62**, 268 (1989).